

Communication Compartments in the Gastrulating Mouse Embryo

Ghulam H. Kalimi and Cecilia W. Lo

Biology Department, University of Pennsylvania, Philadelphia, Pennsylvania 19104

Abstract. We characterized the pattern of gap junctional communication in the 7.5-d mouse embryo (at the primitive streak or gastrulation stage). First we examined the pattern of dye coupling by injecting the fluorescent tracers, Lucifer Yellow or carboxyfluorescein, and monitoring the extent of dye spread. These studies revealed that cells within all three germ layers are well coupled, as the injected dye usually spread rapidly from the site of impalement into the neighboring cells. The dye spread, however, appeared to be restricted at specific regions of the embryo. Further thick section histological analysis revealed little or no dye transfer between germ layers, indicating that each is a separate communication compartment. The pattern of dye movement within the embryonic ectoderm and mesoderm further suggested that cells in each of these germ layers may be subdivided into smaller communication compartments, the most striking of which are a number of "box-like" domains. Such compartments,

unlike the restrictions observed between germ layers, are consistently only partially restrictive. In light of these results, we further monitored ionic coupling to determine if some coupling might nevertheless persist between germ layers. For these studies, Lucifer Yellow was coinjected while ionic coupling was monitored. The injected Lucifer Yellow facilitated the identification of the impalement sites, both in the live specimen and in thick sections in the subsequent histological analysis. By using this approach, all three germ layers were shown to be ionically coupled, indicating that gap junctional communication is maintained across the otherwise dye-uncoupled "germ layer compartments." Thus our results demonstrate that partially restrictive communication compartments are associated with the delamination of germ layers in the gastrulating mouse embryo. The spatial distribution of these compartments are consistent with a possible role in the underlying development.

IN multicellular organisms, the ability to develop and function as an integrated whole often depends on information exchanged through cell-cell contacts. The gap junction is a specialized intercellular contact of particular relevance in this regard. Gap junctions are found between cells of most embryonic and adult tissues (Loewenstein, 1979), and their presence can be detected functionally by monitoring the intercellular passage of electrical currents (ionic coupling) or fluorescent dye (dye coupling). These and other studies have revealed that gap junctions contain intramembranous channels that span the lipid bilayers of two adjacent cells and thus allow the passive exchange of ions and molecules of up to 1,000 D (Loewenstein, 1979). Given these properties, it has been suggested that this form of cell-cell interaction may play an important role in development, perhaps in organizing pattern—such as in laying down the body plan of a developing organism (Wolpert, 1978; Loewenstein, 1979; Caveney, 1985; Lo, 1985).

In the first study describing the presence of "low resistance" or gap junctional contacts, cells of the squid embryo were reported to be ionically coupled (Potter et al., 1966). It was further found that with development, coupling was lost between the yolk cell and cells of the embryonic tissues. Gap junctional communication has since been studied in embryos

of various species, including molluscs (De Laat et al., 1980; Dorresteyn et al., 1983), amphibians (Slack and Palmer, 1969; Warner, 1973), *Fundulus* (Bennett et al., 1978; Kimmel et al., 1984), chick (Sheridan, 1968), and the mouse (Lo and Gilula, 1979a, b). These studies generally show that as in the case of the squid embryo, coupling that is turned on early in development, becomes gradually restricted as a function of development.

Our studies have been focused on the possible role of gap junctional communication in regulating early mammalian embryogenesis. Previously we found that in mouse embryos, gap junctional communication was first turned on at the late 8-cell stage, at which time all the blastomeres become linked via these channels (Lo and Gilula, 1979a). Further analysis of blastocysts hatched and implanted in vitro revealed that this coupling broke down shortly after implantation. Initially dye coupling was lost between the inner cell mass and the trophoblast cells, but with continued in vitro development, to the equivalent of 6.5 d of gestation, dye coupling became further restricted to specific clusters of cells in the inner cell mass (Lo and Gilula, 1979b). The term "communication compartments" was used to describe these discrete domains of cells that are well coupled to each other but uncoupled or poorly coupled to cells beyond a defined boundary. The tem-

poral and spatial distribution of these compartments supported the notion that gap junctional communication may play a role in regulating the ongoing development.

In this study, we further characterized the pattern of gap junctional communication in the 7.5-d mouse embryo, that is embryos at the mid to late gastrulation stage of development (also referred to as the egg cylinder embryo). This stage of development is of particular interest as it is at this time that the overall body plan of the mammalian embryo is laid down. This includes the establishment of separate germ layers, the specification of axial polarity (posterior corresponding to the origin of primitive streak), and the formation of the various extraembryonic tissues comprising the placenta and the yolk sac membranes (Beddington, 1983; Hogan et al., 1986). Thus this is a critical window of time during which many of the important decisions are made in mammalian patterning. Therefore, our hope is that these studies might provide insights into the possible role of gap junctional communication in regulating early mammalian pattern formation.

Materials and Methods

Mating of Mice

Female CD-1 mice (Charles River Breeding Laboratories, Wilmington, MA) 6–8 wk of age were mated with Sjl/J male mice (Jackson Laboratory, Bar Harbor, ME). The day that a vaginal plug was found was considered as day 1 of pregnancy. To obtain embryos at approximately the same developmental stage, pregnant females were killed at 7.5 d of gestation between 11 am and 1 pm. As mammalian development is naturally asynchronous, the embryos usually exhibited some variation in size and extent of development, even amongst littermates. For all Lucifer Yellow-injected embryos and some of the carboxyfluorescein-injected embryos, the precise stage of development was determined by a complete histological analysis of serial sections. A thick section of a typical 7.5-d mouse embryo is illustrated in Fig. 1 (also see Results).

Collection and Immobilization of Embryos

The decidua were dissected out in warm DME containing 12.5 mM Hepes buffer (Gibco, Grand Island, NY) and 10% calf serum. After cutting open the decidua, the parietal endoderm was carefully separated and removed. To prevent movement during microelectrode impalement and dye injection, the embryos were immobilized in a thin layer of agarose. This was carried out by pouring 2–3 ml of 0.8% agarose in saline at 45°C into a 35-mm plastic petri dish, pouring off the excess after 10–15 s, then immediately placing an embryo in the center of the dish. The remaining thin layer of agarose solidified rapidly, thus submerging and immobilizing the bottom part of the embryo, leaving the upper surface free for microelectrode manipulations. After the embryo was immobilized, 1.5 ml of medium (DME, 10% CS, 12.5 mM Hepes buffer) was added to each dish and the dishes were maintained in a 5% CO₂ incubator at 37°C until used for experimentation. Note that at the time of embryo immobilization, the agarose temperature was between 38–42°C. Embryos are likely exposed to this temperature for only a few seconds, as the small volume and large surface area results in rapid cooling of the agarose. Moreover, we determined that the embryo's short term viability and development was not affected by this procedure. This was indicated by the finding that similar to control unembedded embryos, the agarose-embedded embryos exhibited the condensation of somites, the development of a regular heartbeat, and the formation of neural tube after a further 24–48 h of culture (unpublished observations).

Dye Injections

The embryos were used for dye injection within 6 h of collection. Dye injections were performed essentially as described previously (Weir and Lo, 1984). Briefly, microelectrodes were made with Kwik-fil borosilicate glass

tubings of 1.0 mm OD (WPI Instruments, New Haven, CT). Microelectrodes with tip resistance of 15–20 M Ω (when filled with 3.0 M KCl) were backfilled with either a 1.0% solution of dilithium Lucifer Yellow or potassium Lucifer Yellow (Molecular Probes, Inc., Eugene, OR). In some of the initial experiments, a 2.0% solution of 6-carboxyfluorescein (Eastman Kodak Co., Rochester, NY) was also used. Each intracellular impalement was monitored by tracking the membrane potential via the output of an oscilloscope and an audio monitor. A successful intracellular impalement resulted in a distinct potential drop which was visible on the oscilloscope and also clearly audible as a sharp change in the frequency of the audio signal output. In addition, each embryo was visually monitored under darkfield fluorescence. If an impalement was successful, rapid dye fill was observed within a single cell, followed by the slower gradual spread of injected dye into the neighboring cells. After an intracellular impalement was made in the desired region of the embryo, dye injections were carried out for a total of 3–10 min, using 0.5–10-nA current pulses of 0.5-s duration, pulsed once per second. The spread of the fluorescent tracer was monitored using a Leitz inverted epifluorescence microscope and recorded photographically at different time intervals on 35-mm Kodak Tri-X film. The effective ASA of the film was pushed to 800 or 1,600 by developing in Acufine or Diafine developers, respectively (Acufine, Inc., Chicago, IL). At the end of the dye injection period, a phase-fluorescence image (obtained by combining a low level of brightfield and darkfield-fluorescence illumination) was recorded to depict the overall location and extent of dye spread in the whole embryo. In some embryos, multiple impalements were carried out. Immediately after termination of dye injection, fixation was carried out in phosphate buffered formalin at room temperature for Lucifer Yellow-injected embryos or at 4°C for carboxyfluorescein-injected embryos.

Ionic-coupling Studies

For the ionic-coupling studies, microelectrodes were filled with 1.0% K⁺-Lucifer Yellow in 50 mM KCl. This solution was prepared by first dissolving 10 mg K⁺-Lucifer Yellow in 750 μ l of deionized water, and then adding 250 μ l of 200 mM KCl with constant stirring (adding Lucifer Yellow directly to 50 mM or higher concentrations of KCl resulted in the precipitation of the dye). The dye solution was filtered with a 0.2- μ m Centrex filter (Schleicher and Schuell, Inc., Keene, NH), and backfilled into glass micropipettes (15–20 M Ω as measured with 3 M KCl). For these studies, 7.5-d mouse embryos were collected and immobilized using agarose as described above, except that before immobilization the permeability seal of the amniotic cavity was disrupted. This was achieved by either cutting out a small portion (\sim 1/8th) of the embryo from the distal or the lateral sides or by breaking open the visceral endoderm. During intracellular impalements, a constant current of 0.5-s duration and 0.5–1.0-nA intensity was pulsed in one electrode at 0.5-s intervals. After successful cell penetration, these current pulses were stopped and a second microelectrode was similarly impaled into another region of the embryo. Ionic coupling was then monitored in both directions as described previously (Gilula et al., 1978; Lo and Gilula, 1979a; also see the legend to Fig. 8). During the course of each experiment, it is estimated that impalements were held for approximately 4 min, and 10.0-nA current was pulsed from each electrode for a total duration of 1–2 min. Immediately after the electrodes were removed, the embryos were fixed in buffered formalin, and processed for embedding in Spurr's resin (Polysciences, Inc., Warrington, PA) for further histological examination of the location of impalements.

Histology

For the Lucifer Yellow-injected embryos, after fixation the embryos were dehydrated in a graded series of ethanol, infiltrated with and embedded in Spurr's resin (Polysciences, Inc.), and polymerized overnight at 70°C. The Spurr-embedded embryos were each serially sectioned (2–3 μ m thick) with glass knives using a MT 5000 ultramicrotome (Sorvall Instruments Div., Newton, CT). The sections were observed unmounted or after mounting in glycerol. The carboxyfluorescein-injected embryos, after overnight fixation, were embedded in OCT medium (Miles Laboratories, Inc., Elkhart, IN) and frozen in liquid nitrogen vapor. Frozen sections of 8- μ m thickness were then cut and immediately observed after mounting in Histomount (National Diagnostics, Highland Park, NJ). Note that unlike Lucifer Yellow, carboxyfluorescein is not immobilized by the fixative. Hence for such specimens, it was necessary to examine the sections immediately after mounting. All sections were examined in the Leitz epifluorescence microscope and also recorded photographically on 35 mm Tri-X film.

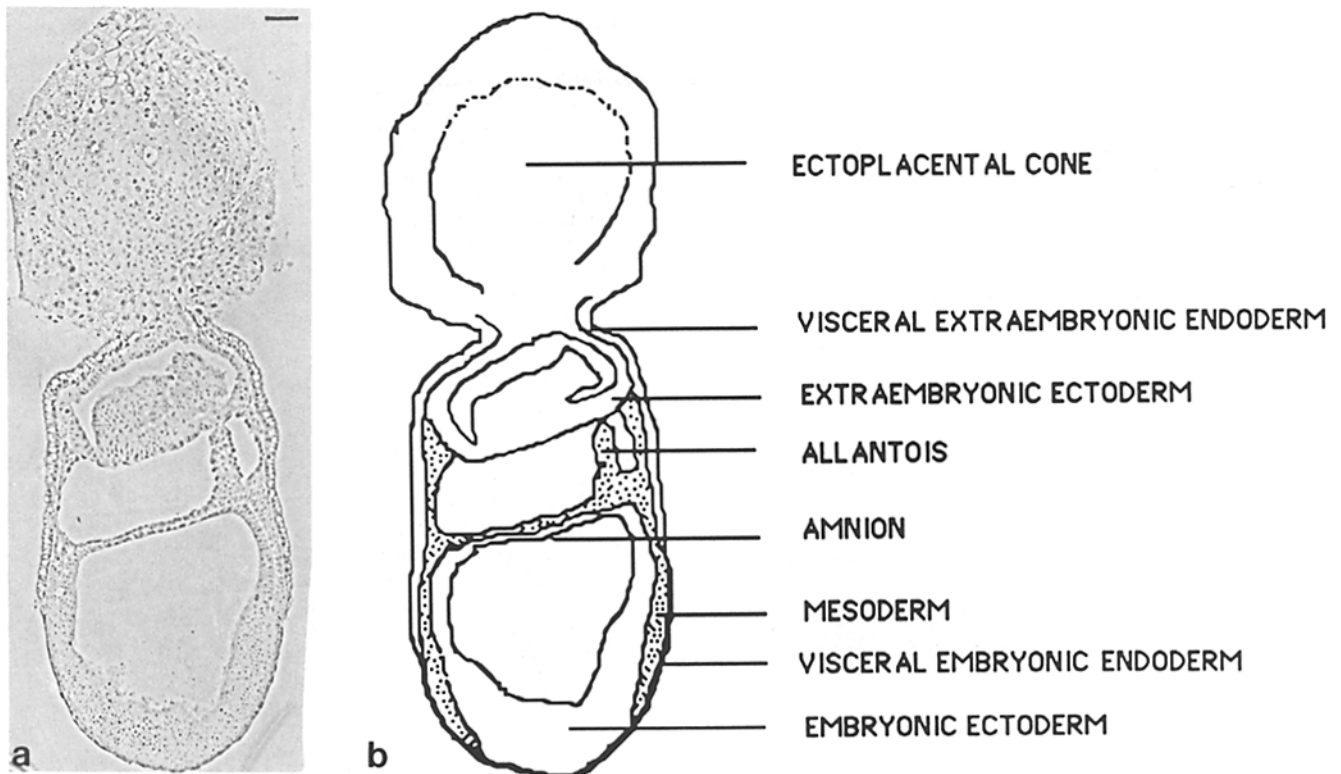


Figure 1. Morphology of the 7.5-d mouse embryo. (a) Saggittal section of a Spurr's embedded 7.5-day mouse embryo. (b) The same section is represented diagrammatically, with the position of different cell types appropriately indicated. Bar, 50 μ m.

Results

The development of mouse embryo begins in earnest with the commencement of gastrulation at the 7th d of gestation. At this stage the embryo has already undergone implantation. This is accompanied by the establishment of an invading placental structure which is extraembryonic in nature. The embryo proper is composed of a hollow cylinder of epithelium referred to as the egg cylinder. Within the egg cylinder, ingression of ectoderm at the primitive streak begins the delamination of a mesoderm layer. Thus in the 7.5-d embryo, there are two distinct embryonic germ layers (Fig. 1), the embryonic ectoderm which is inner most, and a middle layer of mesoderm which is surrounded by a sheet of extraembryonic visceral endoderm (which contributes only to yolk sac development; Hogan et al., 1986). The definitive or embryonic endoderm, which also will be derived from the ectoderm, is not yet detectable at this stage of development.

We characterized the pattern of gap junctional communication in the 7.5-d mouse embryo. Our analysis was focused on examining the pattern of coupling in the egg cylinder proper. First we monitored the extent of dye coupling by using microelectrodes to impale and intracellularly inject the fluorescent tracer carboxyfluorescein. This fluorescent probe was used in the initial studies as it has a high quantum yield (Stewart, 1978) and low molecular mass (376 D). Hence it was an efficient tracer with which to map out the general pattern of gap junctional connectivity within the egg cylinder. These experiments revealed that cells in most

regions of the embryo were well coupled, but generally no dye coupling was observed across germ layers. Of 29 impalements, 18 revealed dye coupling that was apparently restricted to the embryonic ectoderm, 5 in the mesoderm, and 6 in the visceral endoderm. As the mouse embryo at this stage is a complex multicell layered structure, it was necessary to examine the precise intracellular distribution of the fluorescent dye by histological analysis. For this purpose, a subset of the carboxyfluorescein-injected embryos (9 out of 29) were fixed and processed for cryosectioning. These studies indicated a germ layer-restricted pattern of coupling in the egg cylinder embryo.

Given that carboxyfluorescein can not be stabilized by fixation and much of the dye in the specimen diffuses away within a short time after mounting of the cryosections, it was necessary to confirm these findings of restricted dye movement with additional injections of Lucifer Yellow. Unlike carboxyfluorescein, Lucifer Yellow is permanently stabilized by aldehyde fixatives (Stewart, 1978). Moreover, as its fluorescence withstands embedding in the plastic Spurr's resin, it is also possible to obtain superior tissue and cell morphology as compared with the carboxyfluorescein-injected OCT-embedded embryos. Such experiments, in fact, revealed an identical pattern of very limited dye coupling across germ layers (see below).

Restriction of Dye Coupling in the Ectoderm

Two examples of impalements revealing the intracellular

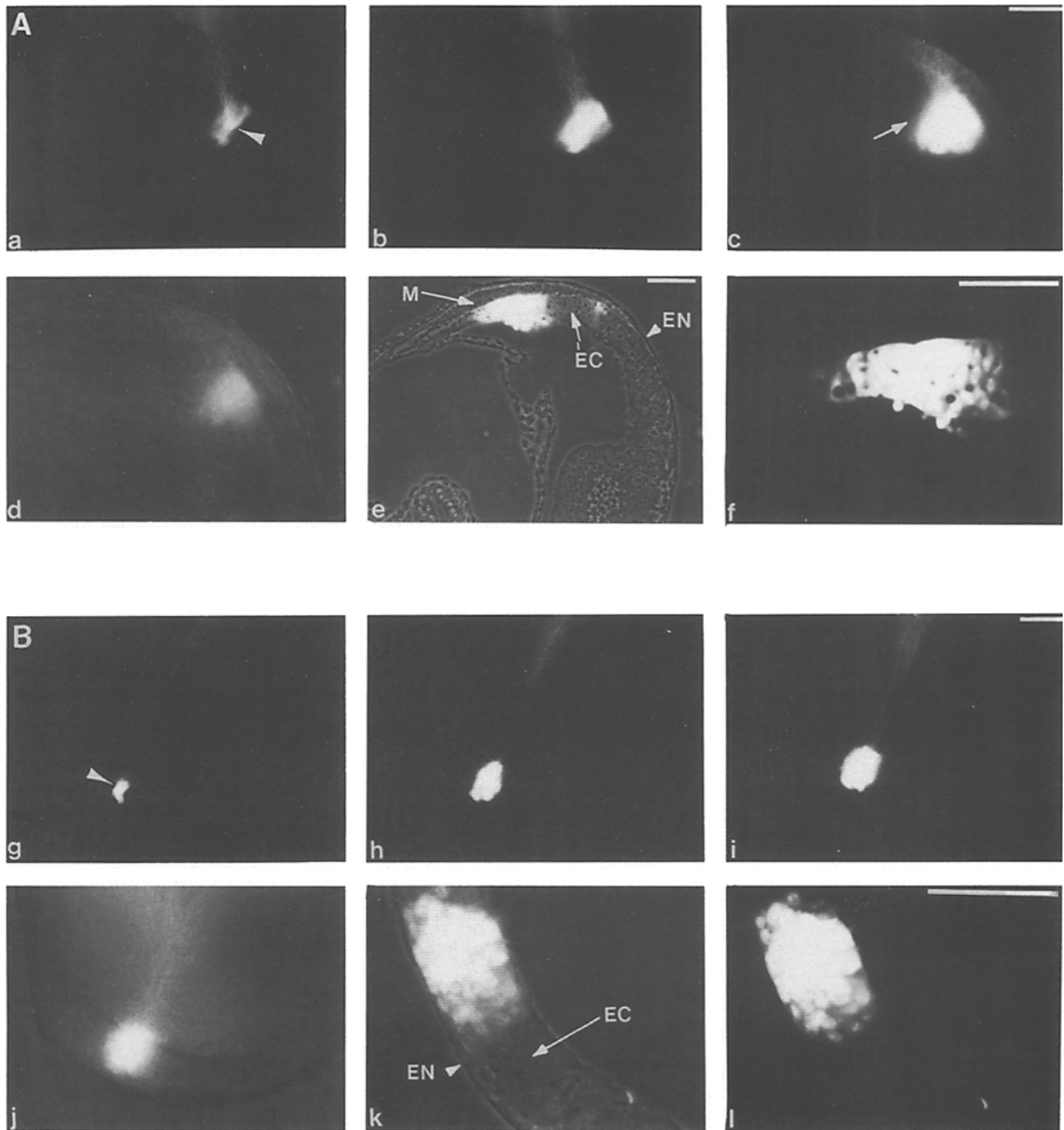


Figure 2. Lucifer Yellow injection into the embryonic ectoderm. (A) Exclusion of dye from the mesoderm layer. A microelectrode was impaled into the embryonic ectoderm of a 7.5-day mouse embryo and Lucifer Yellow was iontophoretically injected intracellularly using a continuous 2-nA hyperpolarizing current pulse of 0.5-s duration at a frequency of once per second. The time course of dye spread is shown by the darkfield-fluorescence images at (a) 15 s, (b) 1.0 min, (c) 2.5 min, and (d) a phase-fluorescence image at 4.0 min after the start of injection. Arrowhead in a denotes the point of impalement. Note that the dye spread was highly asymmetric (see arrow in c). (e) Phase-fluorescence image of a Spurr's section from the above dye-injected embryo. This image demonstrates that the large area of dye spread is in the embryonic ectoderm (EC) layer. No dye is observed in the contiguous mesodermal cells (M). (f) Darkfield-fluorescence image of the same section as shown in (e) but at a higher magnification. (B) Exclusion of dye from the endoderm layer. Dye injection was carried out with an impalement into the embryonic ectoderm of a 7.5-day embryo. The pattern of dye spread is recorded via darkfield-fluorescence at (g) 15 s, (h) 1.5, (i) 3.0, and (j) 4.0 min (phase-fluorescence image) after the start of injection. The arrowhead in g indicates the point of impalement. (k and l) Phase and darkfield fluorescence images of a plastic section from the same embryo. The dye spread is clearly restricted to the embryonic ectoderm (EC) layer, with no dye being transferred to the visceral endodermal cells (EN). Note that in this region of the embryo, the mesoderm layer has not yet formed. Bars, 50 μ m (bar in c and i indicate the magnification in a-d and g-j, respectively).

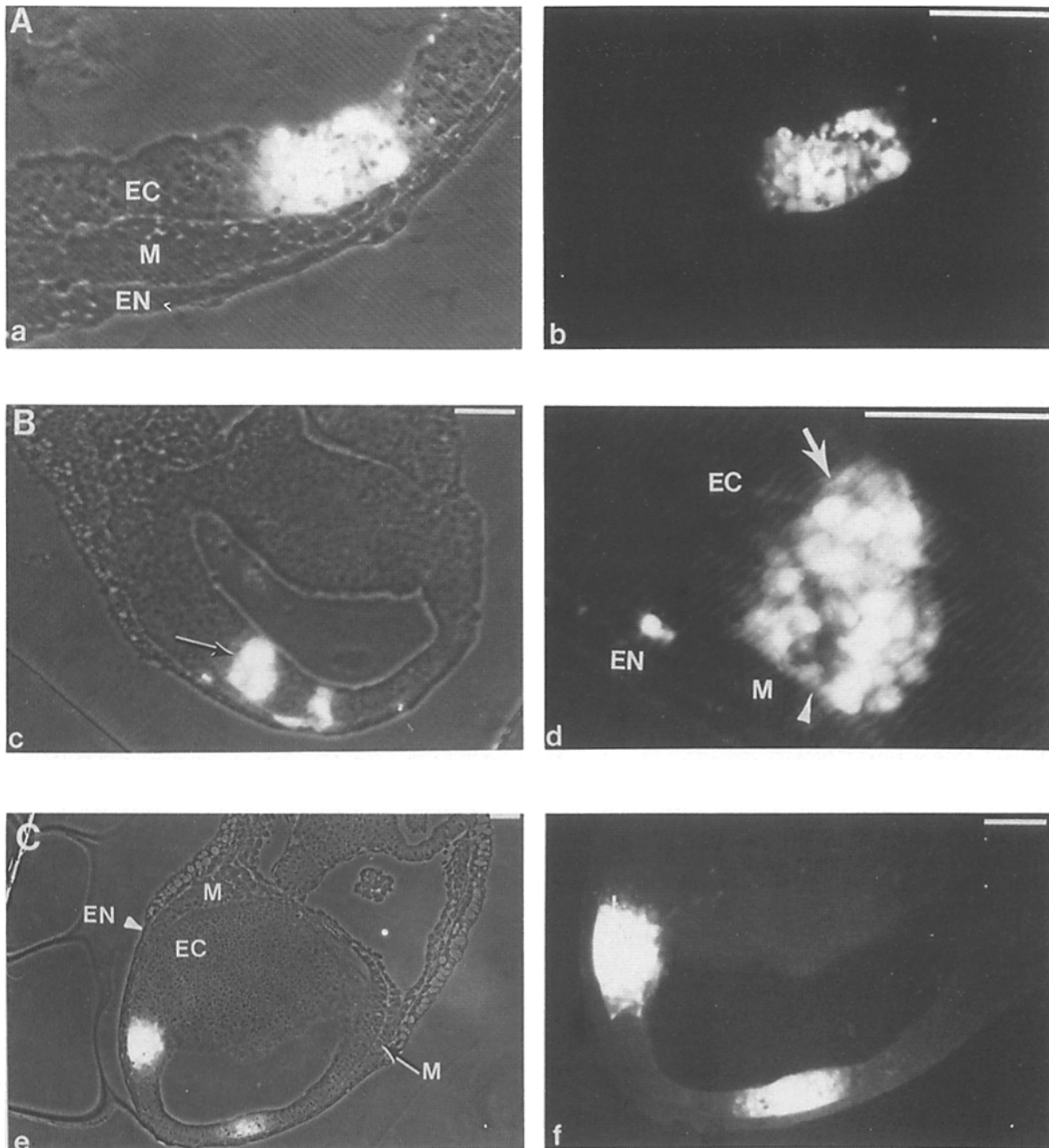


Figure 3. Thick section analysis of dye spread restricted to the embryonic ectoderm of other dye-injected embryos. Illustrated here are thick sections from three other embryos (*A*, *B*, and *C*) injected with Lucifer Yellow. In each case, the injected dye is observed to spread exclusively in the ectoderm (*EC*) layer. Note that in *A* and *B*, Lucifer Yellow is clearly confined to the ectodermal cells, even though the mesodermal cells abut the ectoderm layer (for example, see *arrowhead* in *d*). Also note that in *B*, the pattern of dye spread appears to delineate another restriction boundary as indicated by the black/white arrow in *c* and white arrow in *d*. In embryo *C*, two separate impalements were carried out, each of which resulted in extensive dye spread, but only in the ectoderm layer. This localization can be clearly observed in the phase-fluorescence image in *e*, and more clearly detailed in the darkfield-fluorescence image at higher magnification in *f*. All bars, 50 μm (the magnification of *a* and *b* is indicated by the scale bar in *b*).

spread of Lucifer Yellow in the embryonic ectoderm is illustrated in Fig. 2. In the embryo shown in Fig. 2 *A*, the point of impalement is indicated by a white arrowhead in *a*. Over a period of 2.5 min, Lucifer Yellow was observed to spread extensively. In the phase-fluorescence image in Fig. 2 *A*, *d*, the cluster of fluorescent cells appear to delineate two borders, one corresponding to the separation between the

two germ layers and the other orthogonal to the boundary between germ layers. These boundaries are likely to represent regions where cell-cell communication is either greatly reduced or nonexistent. We refer to these as communication restriction boundaries and cells on either side to be separate communication compartments. Thick section analysis of this embryo after fixation and Spurr's embedding revealed the

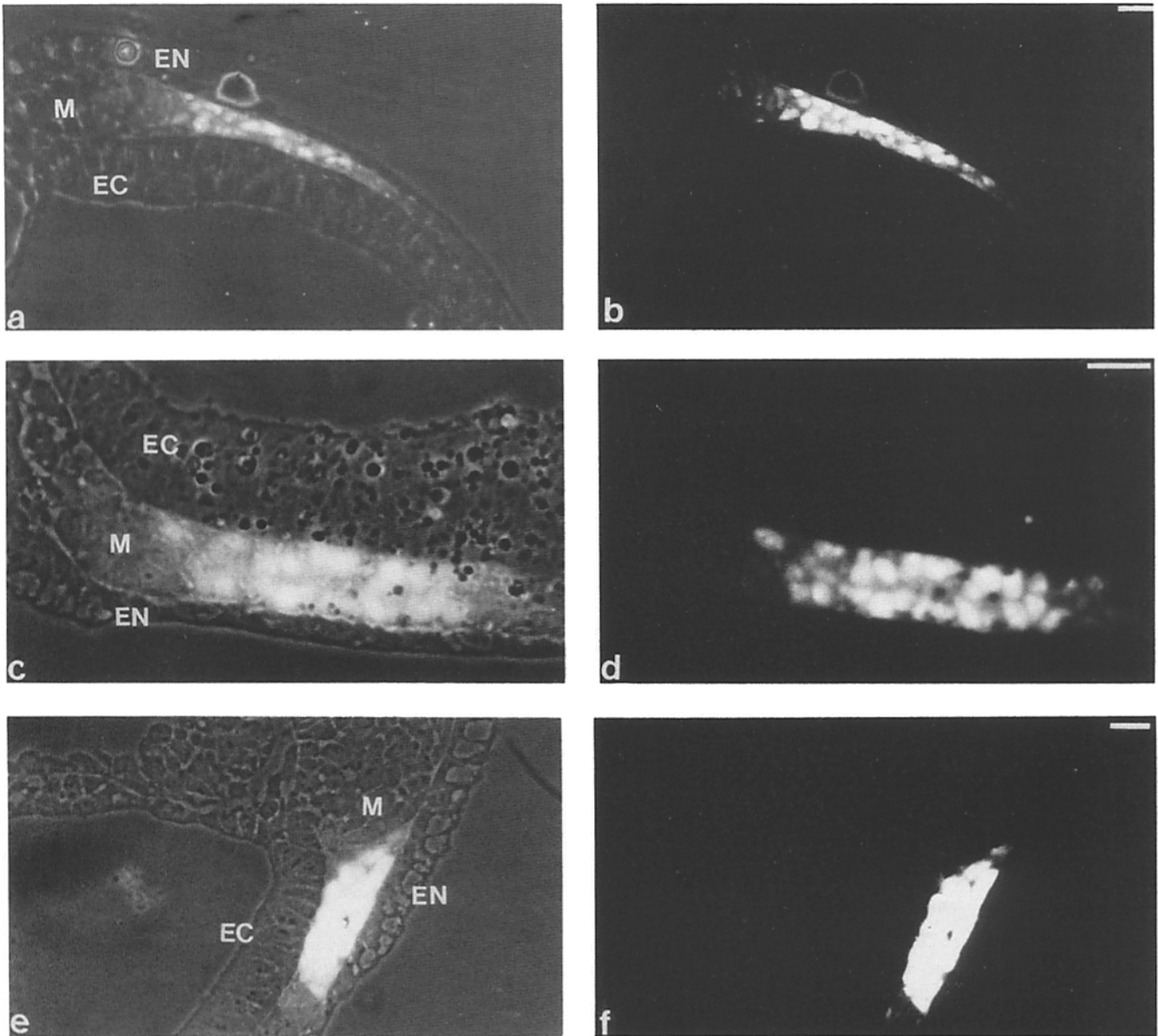


Figure 4. Thick section analysis of embryos impaled in the mesoderm layer. (a-f) Phase-fluorescence (a, c, and e) and their respective darkfield-fluorescence images (b, d, and f) of Spurr's sections from three different embryos impaled and injected with Lucifer Yellow. In each case, the dye spread is restricted to cells of the mesoderm (M) layer, with no dye transfer to cells in the neighboring ectoderm (EC) or endoderm (EN). Bars, 20 μ m.

presence of Lucifer Yellow in the ectoderm, but no dye in the contiguous mesoderm layer (Fig. 2 B, e and f), thus confirming the germ layer-specific restriction in dye coupling. However, due to the plane of sectioning, the second dye restriction border is not visible in this section. Nevertheless, it is worth noting that the dye movement is highly asymmetric, spreading predominantly away from this second border. Thus it is likely that this second border also corresponds to a region of restricted dye spread, but within the ectoderm layer itself (see below for further discussion).

In the second experiment, illustrated in Fig. 2 B, the pattern of dye spread was not easily interpretable in the whole mount (Fig. 2 B, g-j), as the fluorescence image was dis-

torted by the refraction and scattering of light in the multicell-layered embryo. However, with the aid of thick section histology, we determined that the injected dye was localized to the ectoderm layer exclusively (Fig. 2 B, k and l). Note that in this embryo, unlike the impalement in embryo Fig. 2 A, the ectoderm still directly adjoins the visceral endoderm (compare Fig. 2 A, e and B, k). Thus the results of these two experiments indicate that the ectoderm is not dye coupled to cells of either the mesoderm or visceral endoderm layer. Several other examples showing the restriction of dye spread in the ectoderm are further illustrated in Fig. 3. In cases where multiple impalements were carried out into the same embryo, an identical pattern was observed. An exam-

ple of this is shown in Fig. 3 C, in which a single embryo was impaled twice, each revealing an ectoderm-restricted pattern of dye spread.

Restriction of Dye Coupling to the Mesoderm

Impalements into the mesoderm were technically more difficult. This is probably a result of the fact that the mesoderm layer is thinner and its cells are packed more loosely. The dye spread pattern obtained revealed extensive coupling amongst cells of the mesoderm layer, but little or no dye spread into cells of the neighboring embryonic ectoderm or visceral endoderm. Three examples of Lucifer Yellow injections in the mesoderm are shown in Fig. 4. For each embryo, a phase and its corresponding darkfield-fluorescence image is illustrated. Note that the pattern of spotty fluorescence in the darkfield image is a result of the stronger binding of Lucifer Yellow by cell nuclei and does not reflect any discontinuity in the pattern of dye spread. The Lucifer Yellow in the cell cytoplasm can be observed with longer photographic exposures, or by direct visual observation of the specimen.

Multiple Impalements and the Restriction of Dye Coupling in the Three Germ Layers

The germ layer-specific restrictions in dye coupling found in the ectoderm and mesoderm layers were also observed when impalements and dye injections were carried out in the visceral embryonic endoderm. Moreover, all three of these germ layer-specific restrictions can be observed with multiple impalements into a single embryo. One such example of a multiple-impaled embryo is illustrated in Fig. 5. In this case, a single embryo was examined for dye coupling via four successive impalements. The precise distribution of Lucifer Yellow, which is not discernible in the embryo whole mount, is clearly delineated in the thick sections (see Fig. 5, *b*, *d*, *f*, *g*, and *h*). In impalements 1 and 4, dye spread was observed in the ectoderm layer (Fig. 5, *d*, *g*, and *h*), impalement 3 revealed dye spread restricted to the mesoderm layer (Fig. 5 *f*), and impalement 2 exhibited dye spread predominantly in the endoderm layer (Fig. 5 *d*). Note that in this last impalement, a limited amount of dye has spread from the visceral endoderm into the mesoderm layer (see *arrow* in Fig. 5 *d*). As the fluorescence intensity is greater in the endoderm layer, it would indicate that any coupling between the endoderm and mesoderm is probably less efficient than the level of coupling within either germ layer. Such apparent "partial restrictions" have also been observed between the mesoderm/ectoderm and endoderm/ectoderm layers (see Table I).

A summary of our results is tabulated in Table I. From a total of 90 impalements into 56 embryos, 76 show exclusive dye spread within a single germ layer. Of these, 42 were in the ectoderm, 22 in the mesoderm, and 12 in the visceral endoderm layer. These results in conjunction with the carboxyfluorescein data indicate the presence of three boundaries at which dye coupling is restricted: one separating the visceral endoderm/mesoderm, another separating the mesoderm/ectoderm, and a third separating the visceral endoderm/ectoderm (where mesoderm delamination is incomplete). Thus of the 42 Lucifer Yellow impalements in the embryonic ectoderm, 38 delineated the mesoderm/ectoderm boundary,

while 4 delineated the visceral endoderm/ectoderm border (See Fig. 6), and similarly amongst the 12 endoderm impalements, 10 delineated the endoderm/mesoderm border and 2 the endoderm/ectoderm border (Fig. 6). Hence overall, the mesoderm/ectoderm communication restriction boundary has been detected by a composite of 60 separate impalements, the endoderm/mesoderm restriction boundary by 32 impalements, and the ectoderm/endoderm restriction boundary by 6 impalements (see *circled numbers* in Fig. 6).

In a small number of impalements, we also found limited amount of dye spread between cells of adjacent germ layers (i.e., cases of partial restrictions, see Table I). In 90 Lucifer Yellow injections, 12 exhibited some dye transfer between two adjacent germ layers, and in 2 dye coupling was observed between all three germ layers. We believe these examples of apparent dye coupling across germ layers are most likely the result of impalement difficulties and the possible accidental movement of electrode during dye injection. Consistent with this is the fact that in each of the 12 impalements showing dye coupling between germ layers, the injected dye was observed almost entirely within one germ layer, with very few cells exhibiting faint fluorescence in the adjacent germ layer. Given the active nature of primitive streak movement and the associated local breaks in the basal lamina (Soulursh and Revel, 1978; Batten and Haar, 1979; Poelman, 1981; Franke et al., 1983), another possibility can not be completely ruled out; namely, the presence of a low level of coupling between germ layers at a few focal points. In summary on the basis of all of our data, we would conclude that the germ layer-specific restrictions in dye coupling are likely to be complete restrictions.

Compartments within a Germ Layer

Aside from the germ layer-specific restriction in cell-cell communication, the dye spread patterns obtained in the above carboxyfluorescein and Lucifer Yellow injection experiments also revealed smaller domains of restricted dye spread within the ectoderm and mesoderm layers. As in the germ layer-specific restrictions, these compartments are characterized by distinct boundaries exhibiting very sharp discontinuities in fluorescence (for example see Fig. 2 *A* and *B*). However, these restrictions, which are each localized within a single germ layer, do not coincide with any morphological landmark. Some are clearly only partially restricted as indicated by the fact that with continuous injection, the fluorescent tracer consistently spread beyond the compartment boundary. In such instances, a sharp discontinuity in fluorescence is nevertheless maintained for several minutes after the injected dye has moved across the border, thus indicating that cell-cell coupling is less efficient across the border than between cells localized to either side of the border. That such discontinuities in fluorescence intensities do indeed result from a restriction in gap junctional communication is further suggested by the finding that impalements made close to a putative compartment border are characterized by highly asymmetric dye movement, with dye spreading predominantly away from the compartment boundary (see for example Fig. 2 *A*).

Of the additional compartments observed in the ectoderm and mesoderm layer, the most striking are those that appeared rectangular in shape; we refer to these as being "box-

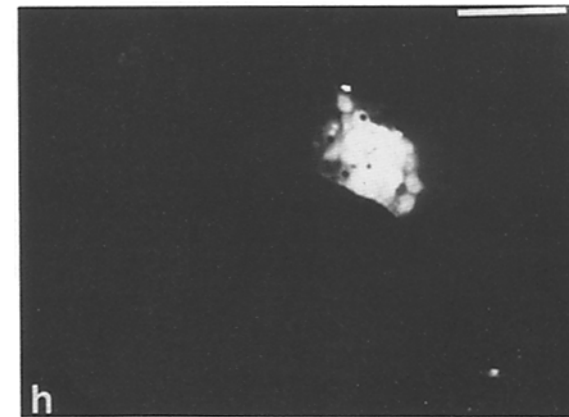
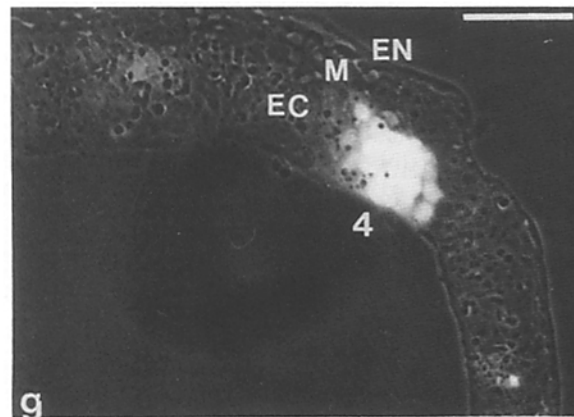
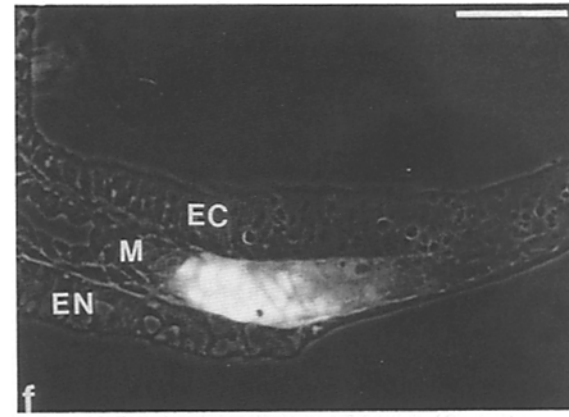
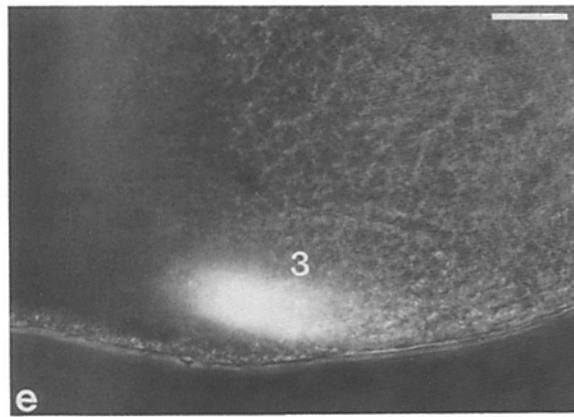
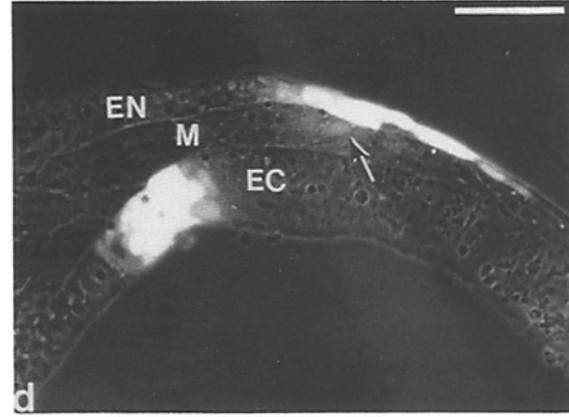
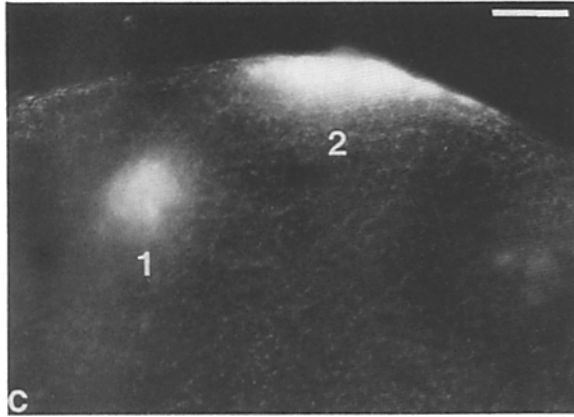
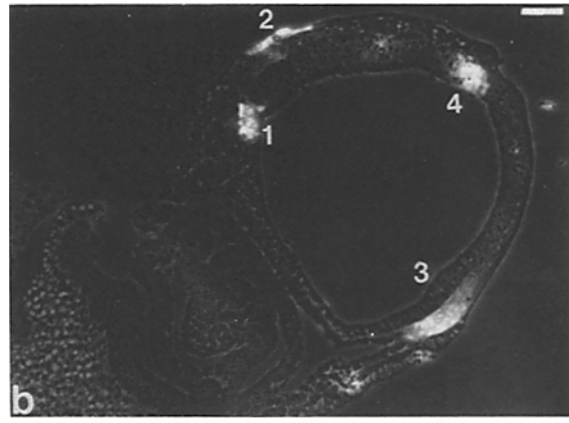
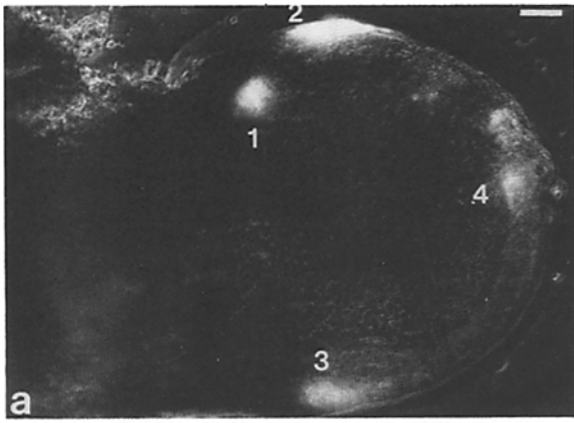


Table I. Lucifer Yellow Injections in the Egg Cylinder of the 7.5-d Mouse Embryo

Region of dye fill	Number of impalements analyzed*
Ectoderm only	42
Mesoderm only	22
Endoderm only	12
Ectoderm and mesoderm	4
Ectoderm and endoderm	2
Mesoderm and endoderm	6
Ectoderm, mesoderm, and endoderm	2
Total	90

* Each embryo was embedded in Spurr's resin and serially sectioned to determine the precise distribution of Lucifer Yellow.

like." Of 23 carboxyfluorescein injections into the embryonic ectoderm/mesoderm layers, 12 impalements delineated box-like domains. Subsequent experiments with Lucifer Yellow revealed such compartments in 6 of 22 impalements into the mesoderm, and 7 of 42 impalements into the embryonic ectoderm. An example of this is shown in the Lucifer Yellow injection experiment in Fig. 7 A. The box-like compartment can be observed both in the phase-fluorescence (Fig. 7 A, a) and darkfield-fluorescence (Fig. 7 A, b) images. Analysis of serial sections of this embryo revealed that the injected dye is present within the ectoderm layer, in a distinct cluster of cells delineated by a very sharp discontinuity in fluorescence (see arrow in Fig. 7 A, b). Note that no obvious change in cell morphology is detectable at the compartment border. These observations suggest that there is a large drop in coupling efficiency between cells on either side of these compartment boundaries. The partial nature of the restriction is indicated by the fact that dye movement across these box-like domains is readily observed when injections are carried out for an extended time interval (between 5 and 7 min). An example of this is shown in Fig. 7 B. In this embryo, dye injection clearly delineated a box-like domain in the ectoderm, but thick section analysis revealed that in some regions, the injected dye has actually spread beyond the compartment boundary. Thus in the thick section of Fig. 7 B, d, some Lucifer Yellow can be seen in the endoderm layer (see arrow in inset of Fig. 7 B, d). In a different section through the same embryo, a small amount of dye also can be seen in the ectoderm layer, beyond the limits of the box-like domain (Fig. 7 B, e and f). When successive impalements were made within

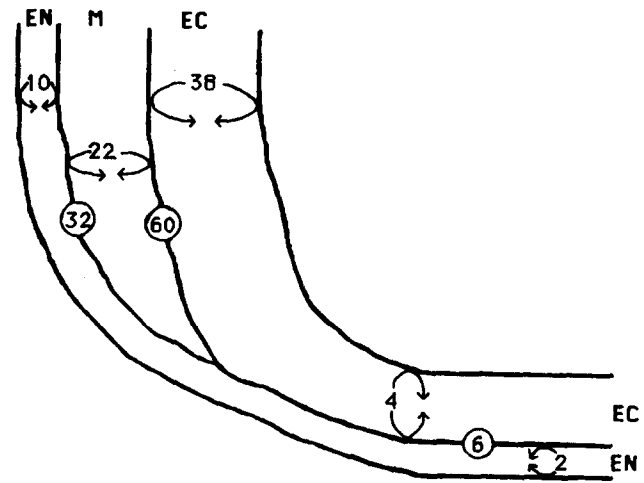


Figure 6. Restrictions in Lucifer Yellow dye coupling in the embryonic germ layers. This diagram schematically summarizes all the data obtained with Lucifer Yellow injections which demonstrated the germ layer-specific restriction in dye coupling. Numbers bracketed by curved arrows denote the number of separate impalements in which dye spread was confined to a single germ layer. The encircled numbers represent the total number of impalements that delineated each of the germ layer-specific communication restriction boundaries. These numbers represent a composite of impalements made on either side of the respective borders. Note that the lower part of the diagram summarizes the data for impalements which delineated the ectoderm/visceral endoderm restriction, that is representing impalements into those regions of the embryo where the mesoderm has not yet formed. EC, embryonic ectoderm; EN, visceral endoderm; M, mesoderm.

a single embryo, several rectangular dye-filled domains can be observed; an example of this is shown in Fig. 7 C. In this embryo, two box-like compartments were delineated and they were separated by a dye-excluded domain of about equal size. In this case, the injected dye also has begun to move beyond the confines of the box-like domains. Thus, unlike the germ-layer restrictions, these box-like compartments consistently exhibited a low level of dye coupling across their compartment borders.

Ionic Coupling between Germ Layers

In light of the partial nature of the box-like compartments, we further examined if a low level of coupling might persist between germ layers; one that might be more easily detected by monitoring for ionic coupling. For this study, impale-

Figure 5. Dye spread pattern obtained with multiple impalements into a single embryo. Lucifer Yellow injections were carried out via multiple impalements into a single 7.5-day mouse embryo. (a) Phase-fluorescence image of the embryo after completion of dye injection and fixation. The four impalements which resulted in extensive dye spread are labeled as 1, 2, 3, and 4. Impalement 1 is located in the ectoderm layer, impalement 2 in the visceral embryonic endoderm layer, impalement 3 in the mesoderm layer, and impalement 4 in the ectoderm layer at the distal tip of the embryo. Note that the other two small patches of fluorescence near impalement 4 resulted from other impalement attempts that were not successful. (b) Phase-fluorescence image of a section from the same dye-injected embryo. The precise distribution of the Lucifer Yellow dye can be clearly observed in this section, and other sections illustrated at higher magnification below. (c-h) Phase-fluorescence and darkfield-fluorescence images of thick sections at higher magnification. For impalements 1 and 2 (see c and d), thick section analysis revealed dye spread mainly within the ectoderm (EC) and visceral endoderm (EN) layers, respectively. However, a limited amount of dye transfer from the endoderm to the mesoderm layer can be observed with impalement 2 (see arrow in d). For impalements 3 (e and f), and 4 (g and h), the injected Lucifer Yellow dye is limited to the mesoderm (M) and ectoderm (EC) layers, respectively. Bars, 50 μ m.

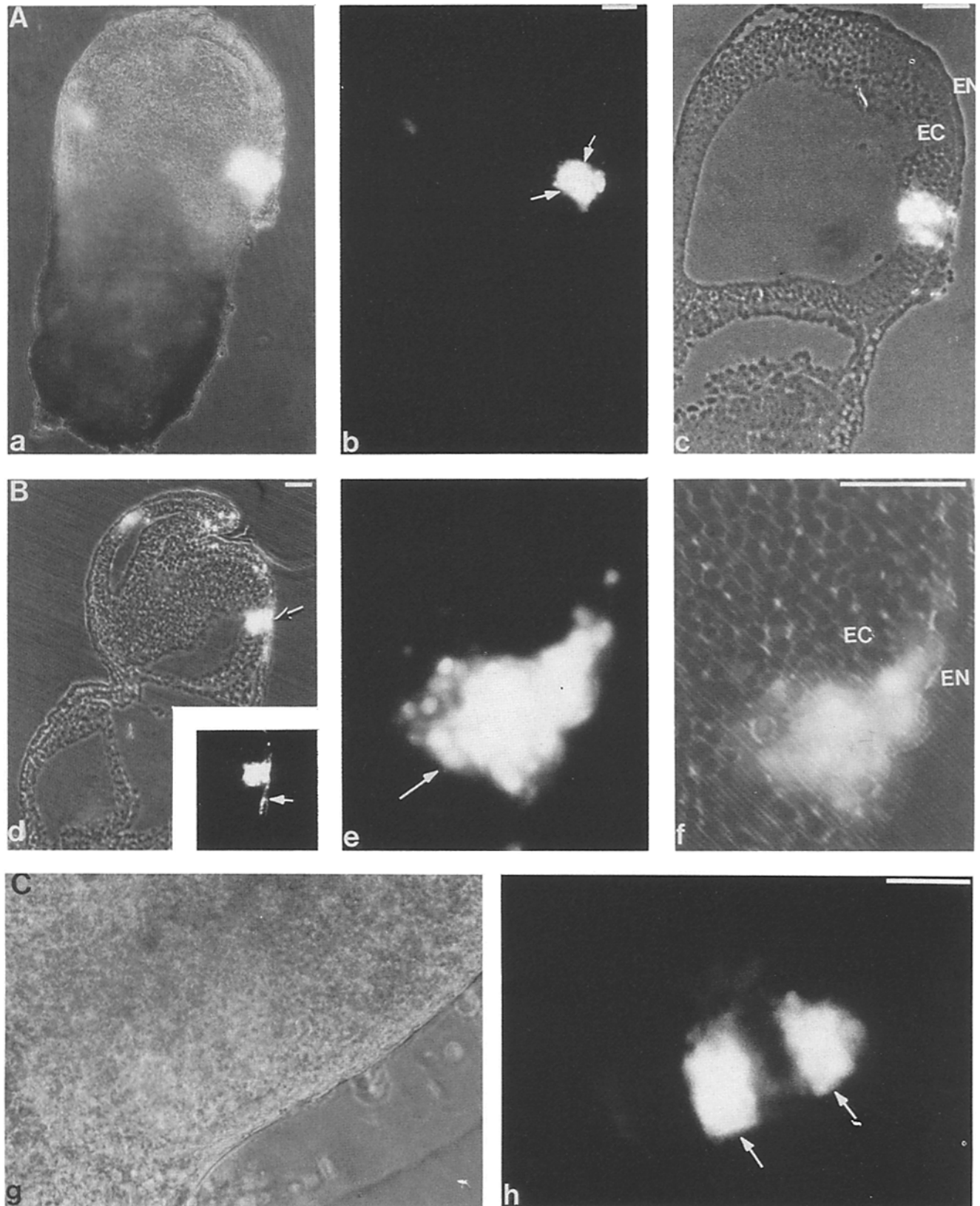


Figure 7. Box-like compartments within a single germ layer. (A) Box-like compartments in the ectoderm. A box-like dye-filled region can be observed in the phase-fluorescence (a), and darkfield-fluorescence (b) images of an intact embryo. A thick section (c) from the same embryo confirmed the presence of the box-like compartment in the ectoderm layer. Note the sharp discontinuity in fluorescence delineating the boundaries of this dye-filled region (see arrows in b). (B) The partial nature of communication restriction associated with the box-like compartments. Phase-fluorescence (d) and darkfield-fluorescence (d, inset) images of a section from another dye-injected embryo reveal a similar box-like compartment (see arrow). The partial nature of the restriction in cell-cell coupling is indicated by the limited amount

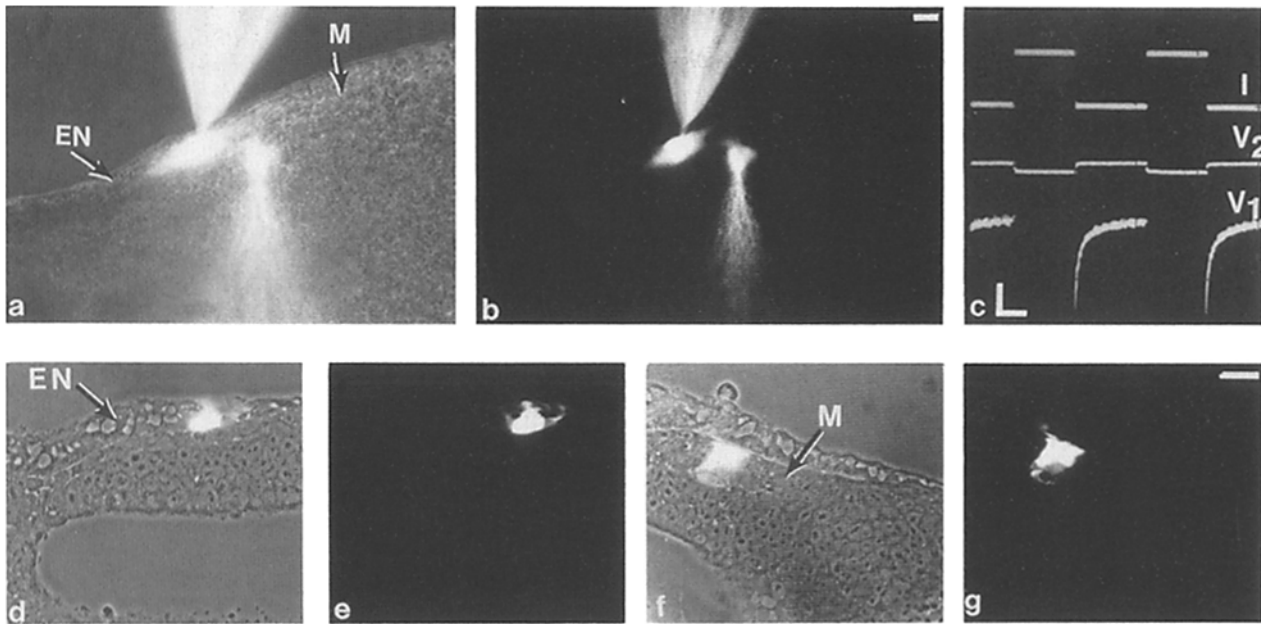


Figure 8. Ionic coupling between cells of the visceral endoderm and mesoderm. Two microelectrodes (filled with 1% K^+ -Lucifer Yellow in 50 mM KCl) were impaled, one into a cell in the visceral endoderm and the other into a cell in the mesoderm layer of a 7.5-d mouse embryo. Continuous current pulses of 10 nA and 0.5-s duration were passed at a frequency of once per second for ~ 2 min, first in the endodermal cell and then the mesodermal cell. The current pulses and the voltage (V_1 and V_2) deflections in each cell were recorded on the oscilloscope, revealing the presence of ionic coupling with current pulsed in either direction. The passage of current also resulted in the injection of Lucifer Yellow, thus allowing the region of impalement to be visualized. Over the 2–4-min total duration of the experiment, the injected dye was also seen to be transferred to adjacent cells. At the end of the experiment, the embryo was fixed, embedded in Spurr's resin, and further analyzed by thick section histology to precisely localize the site of impalements. (a and b) Phase-fluorescence (a) and darkfield-fluorescence (b) images of microelectrode impalements into a 7.5-d mouse embryo. Note that the position of each impalement is clearly delineated by the fluorescent outline of the microelectrode. The two microelectrodes appeared to have been impaled into the endoderm (EN) and mesoderm (M) layer, respectively (also see below). (c) The oscilloscope recording show the presence of ionic coupling between the two impaled cells. Thus as current (I) is pulsed into the endodermal cell, a voltage deflection (V_1) is recorded in that cell, and also simultaneously, in the mesodermal cell (V_2). The vertical bar represents 5 nA/5 mV, and the horizontal bar represents 250 ms. (d–g) Sections from the same embryo. Phase-fluorescence (d and f) and darkfield-fluorescence (e and g) images of two sections showing the presence of fluorescent dye in cells of the endoderm (d and e) and mesoderm (f and g). This analysis confirms the location of one impalement in the mesoderm, and the other in the visceral endoderm. The magnifications in a and b is shown by the scale bar in b, in d–g as shown by the scale bar in g. Bar, 20 μ m.

ments were carried out with microelectrodes filled with 3 M KCl (30–40 M Ω). These electrodes provided stable intracellular impalements with membrane potentials of -10 to -40 mV. With impalements into cells of apparently different germ layers, ionic coupling was readily detected. However, because of the multilayered nature of the embryo, the precise position of impalements remained ambiguous. To circumvent this difficulty, further impalements were carried out with microelectrodes containing K^+ -Lucifer Yellow in 50 mM KCl (prepared as described in Materials and Methods). This was found to be suitable for monitoring ionic coupling and at the same time, permitted the marking of the impaled cell. Moreover, as the injected dye also spread into some of the neighboring cells during the course of the experiment,

this further facilitated the in situ observation and histological analysis of the impalement site. In cases of successful impalements, a membrane potential of -10 to -30 mV was observed and the impaled cell also became strongly fluorescent when observed in darkfield. Impalements into the same and between different germ layers revealed ionic coupling across all three germ layers (see Fig. 11), but the degree of coupling detected was variable, with the highest level observed between cells of the same germ layer. Given the complex geometry of the embryo, it was not possible to quantitate or further evaluate the apparent regional differences in the degree of ionic coupling.

An example of impalements showing the presence of ionic coupling between cells of the visceral endoderm and meso-

of dye spread into the endoderm layer (see *white arrow* in *inset*). This rectangular box-like region is more clearly observed in another thick section at higher magnification in *e* and *f*. Note that in this section, only one of the two borders is visible (see *arrow* in *e*) as the Lucifer Yellow again has clearly spread beyond the confines of the compartment border. (C) Multiple box-like compartments in the ectoderm. Two separate impalements were carried out in the ectoderm. The dye spread pattern delineated two box-like regions (see *arrows* in *h*) with distinct boundaries of restricted dye spread. Note that these boundaries are only partially restricted as some dye has clearly spread beyond the boundaries of the box-like domains. Bars, 50 μ m (the magnification in *a* and *b* is indicated by the scale bar in *a*, in *e* and *f* by the scale bar in *f*, and in *g* and *h* by the scale bar in *h*).

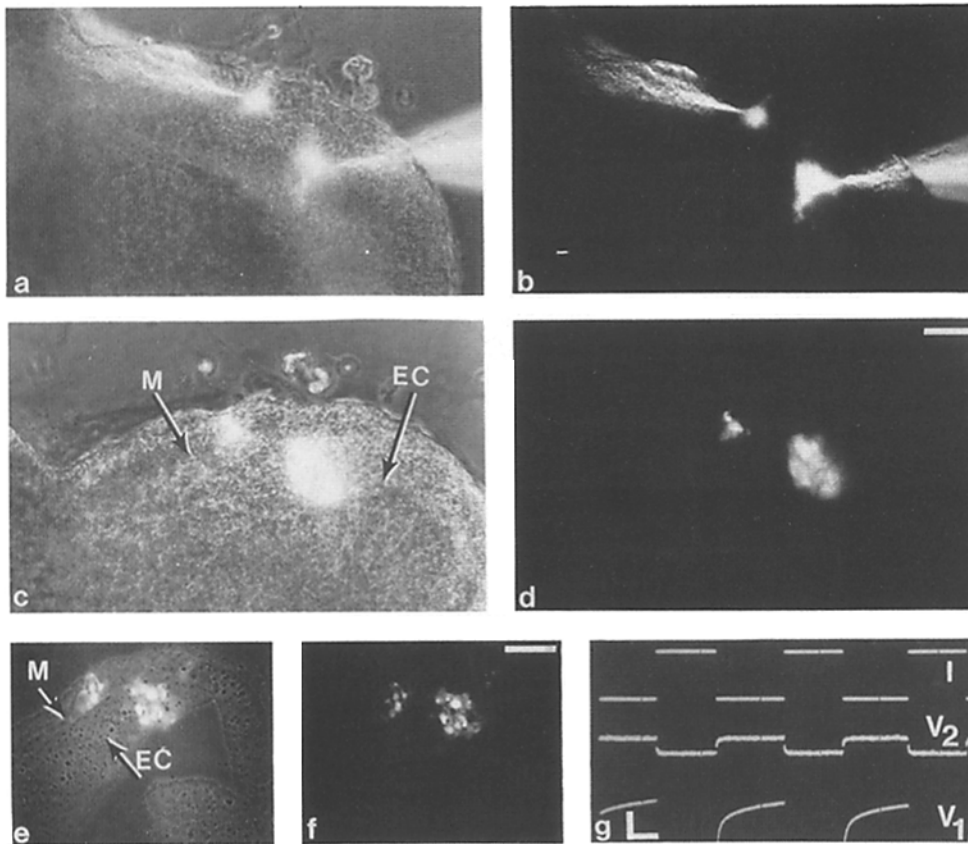


Figure 9. Ionic coupling between cells of the embryonic ectoderm and mesoderm. Microelectrode impalements were carried out in the embryonic ectoderm and mesoderm to determine if these two germ layers were ionically coupled. This experiment was performed as described for the impalements in Fig. 8. (a and b) Phase-fluorescence (a) and darkfield-fluorescence (b) images of a 7.5-d embryo showing the location of the two impalements, with one microelectrode in the embryonic ectoderm and the other in the mesoderm layer. (c and d) Phase-fluorescence (c) and darkfield-fluorescence (d) images of the same embryo after removal of the microelectrodes and fixation with formaldehyde. (e and f) Phase-fluorescence (e) and darkfield-fluorescence (f) images of a section from the same embryo, confirming the location of the two impalements—one being in the ectoderm (EC) and the other in the mesoderm (M) layer. (g) The oscilloscope

recording show the presence of ionic coupling between the ectodermal and mesodermal impalements. Thus as current (I) was pulsed into the ectodermal cell (V_1), a simultaneous voltage deflection was recorded in the mesodermal cell (V_2). The vertical bar represents 5 nA/5 mV and the horizontal bar represents 250 ms. Magnifications in *a-d* are indicated by the bar in *d*, and in *e* and *f* by the bar in *f*. Bar, 50 μ m.

derm is illustrated in Fig. 8. The two regions of impalements were clearly delineated by the Lucifer Yellow in the intact embryo (Fig. 8, *a* and *b*). Subsequent thick section analysis identified the two impalements as being in the endoderm and mesoderm, respectively (Fig. 8, *d-g*). As can be seen from the oscilloscope traces, ionic coupling was detected between these two sites of impalement (Fig. 8 *c*). Another example showing the presence of ionic coupling between the embryonic ectoderm and mesoderm is illustrated in Fig. 9. The phase and darkfield fluorescence images before (Fig. 9, *a* and *b*) and after (Fig. 9, *c* and *d*) fixation, revealed two fluorescent patches corresponding to the two regions of impalement. Subsequent thick section analysis demonstrated that the impalements were in the mesoderm and ectoderm layer, respectively. As in the previous example, ionic coupling was clearly detected across the two germ layers (Fig. 9 *g*). Similar experiments also revealed the presence of ionic coupling across the visceral endoderm and ectoderm layers (Fig. 10). Note that in this case, the degree of coupling detected (see Fig. 10 *d*) was apparently of a smaller magnitude, perhaps reflecting separation of the ectoderm and endoderm by the intervening mesoderm layer. This might account for the finding in one experiment, of no coupling between the visceral endoderm and ectoderm layers.

In summary ionic coupling was monitored with 42 pairs of impalements in 42 embryos, and except for one instance (as mentioned above), all were found to be ionically coupled

(see summary in Fig. 11). These results demonstrate that even though dye coupling is restricted between germ layers, there is nonetheless a detectable level of gap junctional communication between cell of all three germ layers.

Discussion

The results of our study revealed that the gastrulating 7.5-d mouse embryo is well coupled. This is consistent with previous ultrastructural studies which demonstrated the presence of gap junctions in all three germ layers (Batten and Haar, 1979; Franke et al., 1983). Our data also revealed that the 7.5-d mouse embryo is subdivided into a series of communication compartment domains. Thus using the injection of fluorescent dye tracer we found that each germ layer constituted a separate communication compartment. We also detected in a few cases, an apparent low level of dye coupling between germ layers, indicating that the restriction in coupling may be incomplete or partial in nature. However, as pointed out earlier, in these cases it is likely that the apparent spread of dye may have resulted from the accidental movement of the microelectrode between germ layers. Nevertheless, it is interesting to note that our finding of ionic coupling across all three germ layers would indicate that at least a low level of coupling must be maintained across these dye-delineated compartment borders. This would not be unexpected as extensive cell contacts and even gap junctions have

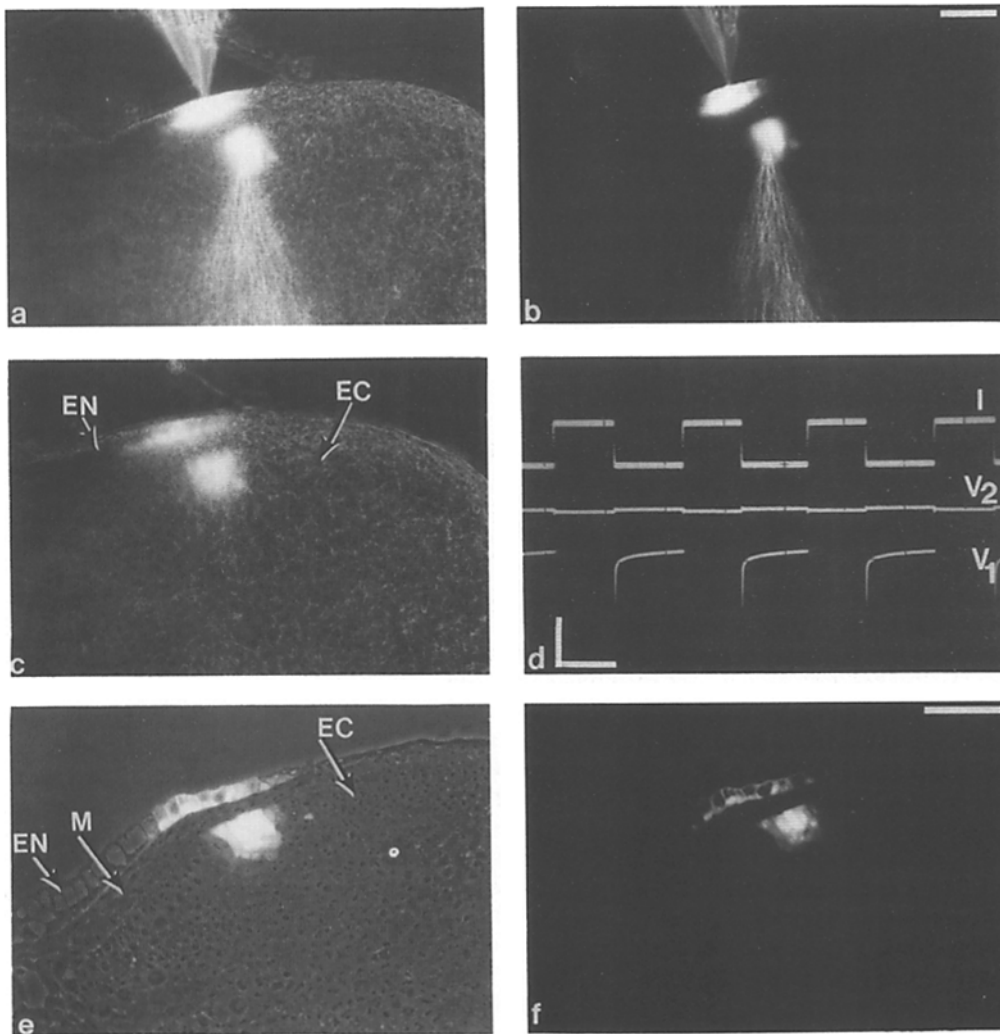


Figure 10. Ionic coupling measurements between cells of the embryonic ectoderm and visceral endoderm. Impalements were performed essentially as described in the legend to Fig. 8 to determine if the ectoderm and endoderm layers were also ionically coupled. (a and b) Phase-fluorescence (a) and darkfield-fluorescence (b) images of a 7.5-d embryo showing the location of two impalements, one in the visceral endoderm and the other in the embryonic ectoderm. (c) Phase-fluorescence image of the same embryo a short time later, and after removal of electrodes and fixation with formaldehyde. (d) The oscilloscope recording shows a low level of coupling across the two impalements. Thus as current (I) is pulsed into the ectoderm cell (V_1), a simultaneous voltage deflection was recorded in the ectodermal cell (V_2). The vertical bar represents 10 nA/10 mV, and the horizontal bar represents 500 ms. (e and f) Phase-fluorescence (e) and darkfield-fluorescence (f) images of a section from the same embryo. The two impalements are distinctly visible as two groups of fluorescent cells, one in the ectoderm (EC) and the other in the endoderm (EN) layer. The magnifications in a-c, are indicated by the bar in b, and in e and f by the bar in f. Bar, 50 μ m.

been observed at the ultrastructural level between cells in the mesoderm and ectoderm layers (Batten and Haar, 1979; Poelman, 1981; Franke et al., 1983). Overall, these observations are in agreement with the previous findings of ionic coupling across dye-filled compartments in the early mouse embryo (implanted in vitro; Lo and Gilula, 1979b) and in the insect segmental hypoderm and imaginal disk epithelium (Warner and Lawrence, 1982; Weir and Lo, 1982; Blennerhasset and Caveney, 1984).

Besides the germ layer-specific restrictions in coupling, we also found that cells within the ectoderm and mesoderm layers are further subdivided into additional dye-filled compartments, the most striking of which are the box-like compartments. In contrast to the germ layer-specific compartments, these restrictions are clearly only partial in nature, as dye spread across a compartment border was readily detected. This is very reminiscent of communication compartments in the *Drosophila* wing imaginal disk (Weir and Lo,

1982, 1984) and in the insect larval hypoderm (Blennerhasset and Caveney, 1984). In the insect system, the restriction in coupling and the partial nature of the restriction appear to result from the presence of a band of cells at the border with a reduced level of coupling (Weir and Lo, 1982; Blennerhasset and Caveney, 1984). At present we have no evidence for such bands of cells in the mouse embryo. Aside from the box-like compartments, our dye injection experiments also revealed the presence of other compartments. One such example is the finding of a semicircular pattern of dye spread (unpublished observations), delineating a compartment consisting of a narrow sector of cells in the embryonic ectoderm at the distal tip of the embryo; the approximate position of the future neural groove (Snell and Stevens, 1966; Morris-Kay, 1981). We are currently carrying out experiments to determine the precise distribution of these and other compartments in the 7.5-d mouse embryo.

Communication compartments have also been described

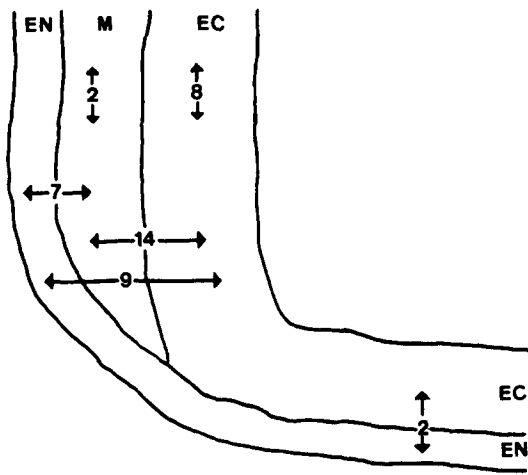


Figure 11. Ionic coupling in the 7.5-d mouse embryo. This diagram summarizes the total number of ionic coupling measurements performed and the germ layer identity of the impaled cells as confirmed by histological analysis of Spurr's sections. Each of the two arrowheads represent the germ layer within which the electrodes were impaled. Ionic coupling was detected in all cases (total 42), except for one pair of impalements in the visceral endoderm and embryonic ectoderm (see text). In some instances, measurements were performed with two impalements into the same germ layer (eight in the ectoderm and two in the mesoderm). The extent of coupling detected was variable, usually being highest with impalements into the same germ layer.

in studies of several other developmental systems in addition to insects and mammals. For example, in the mollusc *Lymnaea*, cells of the embryo are progressively segregated into a number of communication compartments, with the presumptive larval cells being the first to break off into a separate compartment domain (Serras and van den Biggelaar, 1987). In the *Xenopus* embryo, a preferential "dorsal" pathway of dye coupling was detected (Guthrie, 1984) while in the *Fundulus* embryo, at the time of gastrulation, the yolk and the embryo proper became uncoupled with regards to dye transfer (Kimmel et al., 1984). The temporal and spatial organization of these compartmentation events is consistent with gap junctional communication playing a role in the underlying developmental events. Perhaps of greatest significance with regard to this possibility is the fact that in the insect system, communication compartments appear to coincide with "developmental compartments" (Warner and Lawrence, 1982; Weir and Lo, 1982, 1984), which are the basic building blocks for insect pattern regulation (Crick and Lawrence, 1975).

In light of the latter observations, it is interesting to consider what might be the role of gap junctional communication compartments in mammalian development. According to the positional information hypothesis of pattern formation, the developmental fate of any cell is dictated by its coordinates as defined within an information gradient (Wolpert, 1971). Theoretically, gap junctions could play a role in encoding positional information by mediating the formation of appropriate intracellular gradients (Michalke, 1977; Wolpert, 1978; Loewenstein, 1979). Thus in the mouse embryo, the initial uncoupling of the trophoblast giant cells may serve as a way of isolating the embryo proper from communication

with the uterine epithelium (Lo and Gilula, 1979b). This isolation may facilitate the formation of a positional information gradient which can define the overall polarity of the developing embryo, eventually resulting in the subdivision of the embryo into germ layer-specific compartments and subcompartments. Such compartments might then dictate or organize specific morphogenetic events, such as in the case of the box-like compartments, perhaps participate in the mammalian segmentation process. With regard to this latter possibility, it is interesting to note that previously a breakdown in coupling has been observed between newly formed somites and the unsegmented mesoderm in amphibians (Blackshaw and Warner, 1976).

The partial nature of compartment restrictions is also intriguing. Perhaps this could facilitate the coordinate regulation of metabolic activities between compartments or mediate "global" interactions that might play a role in organizing pattern in the developing embryo. Of course, ultimately the elucidation of the role of communication compartments in development will necessitate an understanding of the mechanism(s) through which cell-cell coupling becomes restricted, and in particular, an understanding of how partial restrictions might be achieved. Perhaps this could result from differences in the number of gap junctional channels, or through the modulation of channel permeability. Alternatively, it is possible that there might be different populations of channels with variable sieving properties. The answers to these and other questions must await further studies in the future.

Previously, Lucifer Yellow injections and ionic coupling measurements have been used in many other studies for characterizing the extent of coupling in cells and tissues. Here we show that their combined use may be particularly valuable for defining simultaneously the ionic and dye coupling pattern in complex tissues. Moreover, with this approach, we have the added advantage that the electrode tip can be actively guided to the desired location, and subsequently the impaled cells can be easily identified both during impalement and in the later analysis of the impalement site via thick section histology. This information is indispensable for clarifying how the ionic coupling data might relate to any dye-coupling restriction detected. We will further use this method to examine the ionic-coupling properties of other dye-filled compartments in the gastrulating mouse embryo. We hope that these and other experiments will provide insights into how communication compartments might be functionally related to the underlying gastrulation events in the early mouse embryo.

This work was supported by grant GM 30461 from the National Institutes of Health.

Received for publication 9 September 1987, and in revised form 17 March 1988.

References

- Batten, B. E., and J. L. Haar. 1979. Fine structural differentiation of germ layers in mouse at the time of mesoderm formation. *Anat. Rec.* 194:125-142.
- Beddington, R. 1983. The origin of the foetal tissues during gastrulation in the rodents. *Dev. Mamm.* 5:1-32.
- Bennett, M. V. L., M. E. Spira, and D. C. Spray. 1978. Permeability of gap junctions between embryonic cells of *Fundulus*: a reevaluation. *Dev. Biol.* 65:114-125.
- Blackshaw, S. E., and A. E. Warner. 1976. Low resistance junctions between mesoderm cells during formation of trunk muscles. *J. Physiol.* 255:209-230.
- Blennerhassett, M. G., and S. Caveney. 1984. Separation of developmental

- compartments by a cell type with reduced junctional permeability. *Nature (Lond.)*. 309:361-364.
- Caveney, S. 1985. The role of gap junctions in development. *Annu. Rev. Physiol.* 47:319-335.
- Crick, F. C. H., and P. A. Lawrence. 1975. Compartments and polyclones in insect development. *Science*. 189:340-347.
- De Laat, S. W., L. G. J. Tertoolen, A. W. C. Dorresteyn, and J. A. M. Van den Biggelaar. 1980. Intercellular communication patterns are involved in cell determination in early molluscan development. *Nature (Lond.)*. 287:546-548.
- Dorresteyn, A. W. C., H. A. Wagemaker, S. W. de Laat, and J. A. M. van den Biggelaar. 1983. Dye coupling between blastomeres in early embryos of *Patella vulgata* (Mollusca, gastropoda): Its relevance for cell determination. *Roux's Arch. Dev. Biol.* 192:262-269.
- Franke, W. W., C. Grund, B. W. Jackson, and K. Illmensee. 1983. Formation of cytoskeletal elements during mouse embryogenesis. IV. Ultrastructure of primary mesenchymal cells and their cell-cell interactions. *Differentiation*. 25:121-141.
- Gilula, N. B., M. L. Epstein, and W. H. Beers. 1978. Cell-to-cell communication and ovulation. A Study of the cumulus-oocyte complex. *J. Cell Biol.* 78:58-75.
- Guthrie, S. C. 1984. Patterns of junctional communication in the early amphibian embryo. *Nature (Lond.)*. 311:149-151.
- Hogan, B., F. Constantini, and E. Lacy. 1986. Manipulating the mouse embryo. A laboratory manual. Cold Spring Harbor Laboratory, Cold Spring Harbor, New York. 1-332.
- Kimmel, C. B., D. C. Spray, and M. V. L. Bennett. 1984. Developmental uncoupling between blastoderm and yolk cell in the embryo of the teleost *Fundulus*. *Dev. Biol.* 102:483-487.
- Lo, C. W. 1985. Communication compartmentation and pattern formation in development. In *Gap Junctions*. M. V. L. Bennett and D. C. Spray, editors. Cold Spring Harbor Laboratory, Cold Spring Harbor, New York. 251-264.
- Lo, C. W., and N. B. Gilula. 1979a. Gap junctional communication in the preimplantation mouse embryo. *Cell*. 18:339-409.
- Lo, C. W., and N. B. Gilula. 1979b. Gap junctional communication in the post implantation mouse embryo. *Cell*. 18:411-422.
- Loewenstein, W. R. 1979. Junctional intercellular communication: the cell to cell membrane channel. *Physiol. Rev.* 61:829-913.
- Michalke, W. 1977. A gradient of diffusible substance in a monolayer of cultured cells. *J. Membr. Biol.* 33:1-20.
- Morris-Kay, G. M. 1981. Growth and development of pattern in the cranial neural epithelium of rat embryos during neurulation. *J. Embryol. Exp. Morph.* 65(Suppl):225-241.
- Poelman, R. E. 1981. The formation of embryonic mesoderm in the early post-implantation mouse embryo. *Anat. Embryol.* 162:29-40.
- Potter, D. D., E. J. Furshpan, and E. S. Lennox. 1966. Connections between cells of the developing squid as revealed by electrophysiological methods. *Proc. Natl. Acad. Sci. USA*. 55:328-335.
- Serras, F., and J. A. M. van den Biggelaar. 1987. Is a mosaic embryo also a mosaic of communication compartments? *Dev. Biol.* 120:132-138.
- Sheridan, J. D. 1968. Electrophysiological evidence for low resistance intercellular junctions in the early chick embryo. *J. Cell Biol.* 37:650-659.
- Slack, C., and J. F. Palmer. 1969. The permeability of intercellular junctions in the early embryo of *Xenopus laevis*, studied with a fluorescent tracer. *Expt. Cell Res.* 55:416-419.
- Snell, G. D., and L. C. Stevens. 1966. Early embryology. In *Biology of the laboratory mouse*. E. L. Green, editor. McGraw-Hill, Inc., New York. 205-245.
- Solursh, M., and J. P. Revel. 1978. A SEM study of cell shape and cell appendages in the primitive streak region of rat and chick embryos. *Differentiation*. 11:185-190.
- Stewart, W. W. 1978. Functional connections between cells as revealed by dye-coupling with a highly fluorescent naphthalimide tracer. *Cell*. 14:741-759.
- Warner, A. E. 1973. The electrical properties of the ectoderm in the amphibian embryo during induction and early development of the nervous system. *J. Physiol.* 235:267-286.
- Warner, A. E., and P. A. Lawrence. 1982. Permeability of gap junctions at the segmental border in insect epidermis. *Cell*. 28:243-252.
- Weir, M. P., and C. W. Lo. 1982. Gap junctional communication compartments in the *Drosophila* wing disk. *Proc. Natl. Acad. Sci. USA*. 79:3232-3235.
- Weir, M. P., and C. W. Lo. 1984. Gap junctional communication compartments in the *Drosophila* imaginal disk. *Dev. Biol.* 102:130-146.
- Wolpert, L. 1971. Positional information and pattern formation. *Curr. Top. Dev. Biol.* 6:183-224.
- Wolpert, L. 1978. Gap junctions: channels for communication in development. In *Intercellular junctions and synapses*. J. Feldman, N. D. Gilula, and J. D. Pitts, editors. Chapman & Hall, London. 5:83-94.